

An Apparatus for Noncontact Measurement of Thermal Conductivity by Thermal Radiation Heating¹

K. Hisano²

Thermal radiation calorimetry was applied to measure the thermal conductivity of insulating solid specimens. We consider the system in which a disk-shaped specimen and a flat heater are mounted in a vacuum chamber with the specimen heated on one face by irradiation. A temperature difference between two faces was observed at elevated temperatures under steady-state conditions. An apparatus was developed using a thin graphite sheet as the heater element. Disk-shaped Pyrex glass and Pyroceram specimens, whose surfaces were blackened with colloidal graphite, were used in the measurements. Noncontact temperature measurement was performed using pyrometers and a thermocouple set in the gap between the heater and the specimen. Deviations of the estimated thermal conductivities from the recommended values were about 5% in the temperature range 250 to 800°C.

KEY WORDS: high temperature; noncontact measurement; thermal conductivity; thermal radiation.

1. INTRODUCTION

Calorimetry based on thermal radiation heating has recently been developed for the specific heat capacity measurement of a thin disk-shaped specimen [1, 2]. This calorimetry can also be applied to the thermal conduction measurement. It usually takes a relatively long time, over 1 h, for a specimen to reach an equilibrium state in the case of a conventional method, such as the longitudinal heat flow method. A duration between 10 and 20 min is expected for the specimen to achieve equilibrium at elevated temperatures in the case of the radiation calorimetry.

¹ Paper presented at the Fourth Asian Thermophysical Properties Conference, September 5–8, 1995, Tokyo, Japan.

² Department of Mathematics and Physics, National Defense Academy, Hashirimizu 1-10-20, Yokosuka 239, Japan.

In this paper, a theory and an apparatus to measure the temperature gradient in a specimen by means of a noncontact technique are described. The values of thermal conductivity of Pyrocera 9606 and Pyrex 7740 glass obtained from the experimental results are compared with those published in the literature.

2. THEORETICAL FORMULATION

Let us consider the system shown schematically in Fig. 1 in which a disk-shaped specimen and a heater are mounted in a vacuum chamber with the specimen heated on the front surface by thermal radiation. Assuming that the system is in equilibrium, the power balance at the back surface can be expressed as

$$\lambda A \frac{T_{sa} - T_{sb}}{L} = \sigma A \varepsilon_{sb} (T_{sb}^4 - T_r^4) \quad (1)$$

where λ , σ , ε , L , and A are the thermal conductivity, the Stefan-Boltzmann constant, the emissivity, the specimen thickness, and the specimen surface area, respectively. The subscripts sa, sb, and r refer to the specimen front surface facing the heater, the specimen back surface, and the vacuum chamber, respectively. Power loss due to radiation from the side surface is ignored in the above equation. The thermal conductivity is, therefore, given as

$$\lambda = \frac{\varepsilon_{sb} I_{sb}}{T_{sa} - T_{sb}} L \quad (2)$$

where we have put I_{sb} equal to $\sigma(T_{sb}^4 - T_r^4)$. The physical meaning of I is the radiant power per unit area emitted by the specimen to the chamber wall at room temperature for a perfect absorber.

We need to measure the temperatures of both surfaces of the specimen to obtain the value of thermal conductivity from Eq. (2). T_{sb} can be measured with a pyrometer [1, 2], while T_{sa} can be derived from the heater temperature T_h and the temperature T_t of the thermocouple set in the gap between the heater and the specimen. The energy exchange among the thermocouple junction, the heater, the specimen, and the chamber wall is expressed as

$$e_1(I_h - I_t) = e_2(I_t - I_{sa}) + \dot{Q}_r + e_3 I_t \quad (3)$$

where e_1 , e_2 , and e_3 are coefficients of the emissive (or absorption) power. The definition of these coefficients is based on the theoretical results given

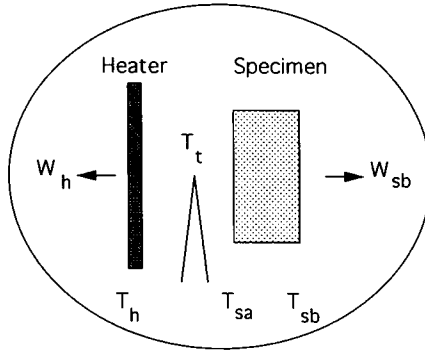


Fig. 1. Schematic of thermal radiation calorimetry. The specimen is heated on one face by thermal radiation from a heater in a vacuum chamber.

by de Burr [3], who discusses the radiant energy exchange between materials kept at different temperatures. In the present system, we consider the exchanges between the junction and the heater, between the junction and the specimen, and between the junction and the chamber wall. It is expected that these coefficients are dependent only on the surface areas and on the emissivities as long as the geometrical relations are the same [1, 2]. \dot{Q}_t is the heat loss per unit time through the thermocouple leads. Equation (3) can be rewritten as

$$I_{sa} = \frac{1}{e_1} \{ (e_1 + e_2 + e_3) I_t - e_1 I_h + \dot{Q}_t \} \tag{4}$$

If we use a high-conductivity specimen where the temperatures of both surfaces can be assumed to be the same, a relation similar to Eq. (4) is obtained with a different set of values for I_{ho} , I_{to} , and I_{so} . Therefore, we have the following relation at $I_t = I_{to}$ (or $T_t = T_{to}$):

$$I_{sa} = I_{so} + \frac{e_1}{e_2} (I_{ho} - I_h) \tag{5}$$

A large cancellation of \dot{Q}_t is expected in the above equation because of the same thermocouple temperature. If the heater radiation power W_h is measured instead of the heater temperature, Eq. (5) can be written as

$$I_{sa} = I_{so} + \left(\frac{1}{G_h} \right) \frac{e_1}{e_2} (W_{ho} - W_h) \tag{6}$$

where $G_h (= W_h/I_h)$ is the gain factor of the electric circuit for the pyrometer. Further, instead of measuring I_{so} , we measure the radiant power W_{so} from the specimen. Therefore, the above equation can be rewritten as

$$W_{sa} = W_{so} + \left(\frac{G_s}{G_h} \right) \frac{e_1}{e_2} (W_{ho} - W_h) \quad (7)$$

Equation (7) implies that noncontact measurement of the front surface temperature facing the heater can be made if the values of proper instrumental quantities of $(G_s/G_h)(e_1/e_2)$, W_{so} , and W_{ho} are known at various temperatures.

3. EXPERIMENTS

A schematic diagram of the experimental arrangement is shown in Fig. 2. The infrared radiant powers from both heater and specimen were measured by thermopile detectors after the radiation passed through light choppers. Figure 3 shows the heater part of the apparatus. The specimen, supported by three thin alumina tubes (1 mm in diameter), was placed at 6 mm above the heater made from a graphite sheet (5 cm square and 0.3 mm in thickness). A Pt-Rh 13% thermocouple (0.1 mm in diameter) was placed in the gap between the heater and the specimen for the measurement of T_1 . The heater part was set in a water-cooled vacuum chamber (20 cm in diameter and 25 cm long) maintained at a vacuum better than 10^{-3} Pa.

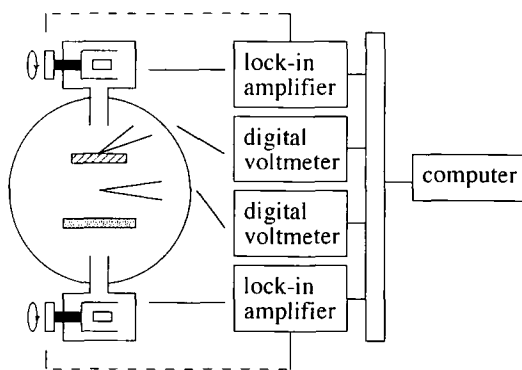


Fig. 2. Schematic diagram for the apparatus for noncontact temperature measurement of the specimen surfaces.

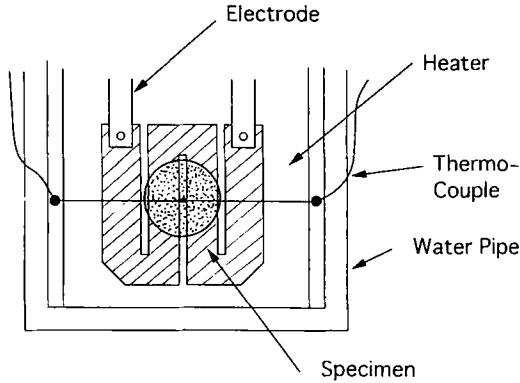


Fig. 3. Heater part of the apparatus. The specimen is suspended 6 mm above the heater. A thermocouple is set in the gap between the heater and the specimen.

Surfaces of the specimens used in the present experiment were blackened with colloidal graphite (Electrodaq 188, Acheson) with a density of $2 \text{ mg} \cdot \text{cm}^{-2}$, yielding a velvet-like surface after evaporation of the acrylic binder above 400°C . The calibration of the surface emissivity was performed by measuring the radiation intensity ratio of the substance to a spray carbon. The emissivity of the spray carbon is known to be 0.85 [4]. Results give the value of 0.95 ± 0.01 from 250 to 800°C for the surface emissivity.

4. RESULTS AND DISCUSSION

4.1. Estimation of $(G_s/G_h)(e_1/e_2)$

Two sets of data for I_s and W_h at certain thermocouple temperature, T_1 , are required so that $(1/G_h)(e_1/e_2)$ can be evaluated from the following relation derived from Eq. (6):

$$\left(\frac{1}{G_h}\right) \frac{e_1}{e_2} = -\frac{I_s - I'_s}{W_h - W'_h} \quad (8)$$

Two disk-shaped copper specimens (25 mm in diameter and 1.5 mm in thickness), on which the thermocouples were attached, were prepared. Both surfaces of one specimen (Cu #1) were blackened with colloidal graphite, while the heater side surface of another specimen (Cu #2) was blackened in the same way as Cu #1 but a polka dot print was made on the back

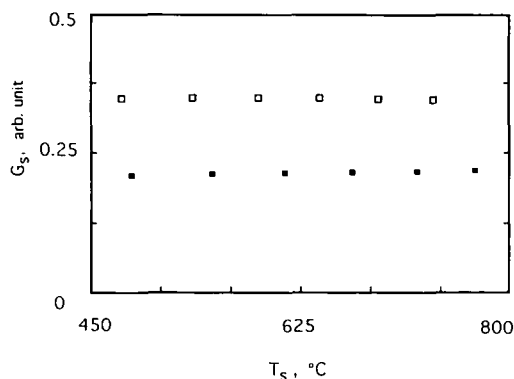


Fig. 4. Temperature dependence of G_s : (□) Cu #1; (■) Cu #2.

surface facing the chamber wall with a density of $0.3 \text{ mg} \cdot \text{cm}^{-2}$ (Aquadaq, Acheson). The measurements of T_s , T_t , W_h , and W_s were performed at various temperatures. No significant temperature gradients in both specimens can be expected because of the high thermal conductivity of copper.

Figure 4 shows $G_s (= W_s/I_s)$ for both specimens at various temperatures. I_s was estimated by use of the thermocouples attached to the specimen. G_s for the Cu #1 specimen is almost independent of temperature, with a value of 0.35, which is much larger than that for the Cu #2

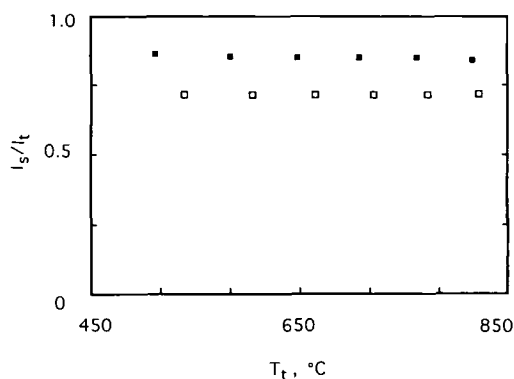


Fig. 5. Temperature dependence of I_s/I_t : (□) Cu #1; (■) Cu #2.

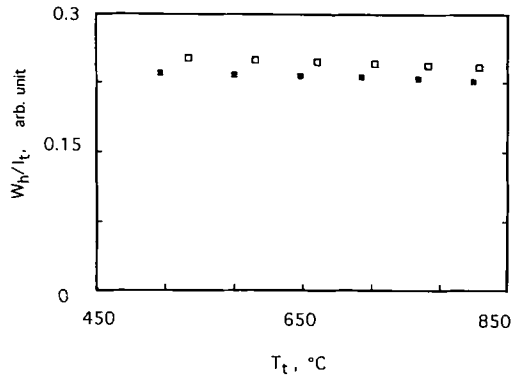


Fig. 6. Temperature dependence of W_h/I_1 : (□) Cu #1; (■) Cu #2.

specimen. Duration for the establishment of the equilibrium state was 12 min after changing the heater current for each temperature in this temperature range. Figure 5 indicates that the Cu #1 specimen keeps a lower temperature than that of the Cu #2 specimen at the same thermocouple temperature T_t , while the heater radiation power for the Cu #1 specimen is larger than that of the Cu #2 specimen as shown in Fig. 6.

A least-squares fit was performed to the Cu #1 data to obtain a continuous analytical function of T_t for I_s and W_h . An average value of 3.5 for $(G_s/G_h)(e_1/e_2)$ was estimated by multiplying G_s by $(1/G_h)(e_1/e_2)$, which is shown in Fig. 7. The measurements were also performed in the temperature range 250 and 500°C. The result also gives a value of 3.5 for $(G_s/G_h)(e_1/e_2)$. The duration for the establishment of the equilibrium state was between 12 and 22 min in this temperature range.

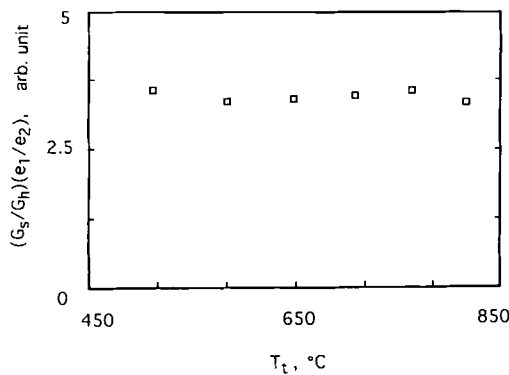


Fig. 7. Temperature dependence of $(G_s/G_h)(e_1/e_2)$.

4.2. Evaluation of Thermal Conductivity

It is also necessary to estimate the values of W_{ho} and W_{so} at various thermocouple temperatures T_1 to obtain the temperature gradient from Eq. (7). A copper specimen, 25 mm in diameter and 0.7 mm in thickness, on which no thermocouple was attached, was prepared for this measurement. Two Pyroceram 9606 specimens, 2.1 and 3.15 mm in thickness, and two Pyrex 9606 specimens, 3 and 5 mm in thickness, were prepared to confirm the validity of Eq. (7), because the thermal conductivity values are well known at various temperatures as reference substances [5, 6]. The diameter of all the specimens is 25 mm. The entire surfaces of these specimens were coated with copper by vacuum evaporation before blackening to keep the radiation loss from the side surface as small as possible.

As a typical example, Table I lists the values of T_1 , W_h , and W_s at equilibrium state for the copper and the 3.15 mm-thick Pyroceram specimens. Each set of values corresponds to the same heater current. The deviation of the radiation powers W_{sa} and W_{sb} of both surfaces from the proper instrumental value of W_{so} is shown in Fig. 8 for the two Pyroceram specimens. The procedure for the data analysis is similar to that for the Cu #1 and Cu #2 specimens. As shown in Fig. 8, the deviation increases for both radiation powers with increasing temperature, which indicates that the temperature difference increases with increasing temperature.

Figure 9 shows the thermal conductivity of the Pyroceram specimens obtained from Eq. (2) together with the temperature difference of the two faces. The specimen temperature was assumed to be $(T_{sa} + T_{sb})/2$. The value of 0.95 was used for ϵ_{sb} . The solid line indicates the temperature dependence of the recommended value. Figure 10 shows the results for the

Table I. Thermocouple Temperature T_1 and Radiant Powers W_h and W_s for Cu and Pyroceram Specimens in the Equilibrium State^a

T_{ho}	T_1	W_{ho}	W_h	W_{so}	W_{sb}
Cu	Pcm	Cu	Pcm	Cu	Pcm
792.5	802.3	16.614	16.817	15.963	15.026
751.2	759.4	14.198	14.367	13.605	12.883
704.5	714.1	11.810	12.064	11.265	10.852
658.2	666.1	9.734	9.929	9.249	8.944
608.7	615.2	7.836	7.980	7.410	7.195
555.8	560.8	6.133	6.234	5.768	5.620

^a Temperatures are in °C and radiant powers are in arbitrary units.

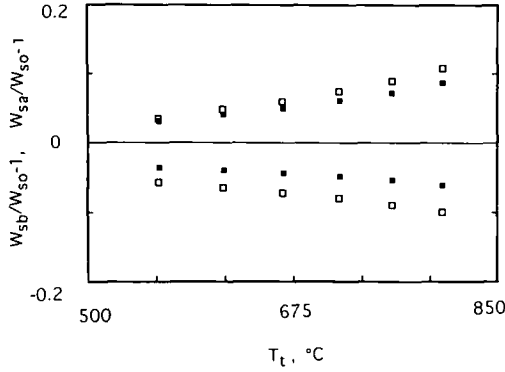


Fig. 8. Temperature dependence of $(W_{sa}/W_{so} - 1)$ and $(W_{sb}/W_{so} - 1)$ for Pyroceram: (□) 3.15 mm thick; (■) 2.10 mm thick.

Pyrex specimens. It is clear from these figures that the temperature difference increases with an increase in temperature. The deviation from the recommended value is about 5%, although the temperature difference seems to be too large to evaluate the thermal conductivity.

The precise evaluation of the errors involved in the results has been difficult in the present investigation. Some major sources of the errors are as follows: the accurate emissivity of blackening substance has not yet been obtained although the value relative to the spray carbon was estimated. The emissivity is not exactly the same for all the specimens. The radiation loss from the side surface becomes large with increasing temperature. \dot{Q}_1 is

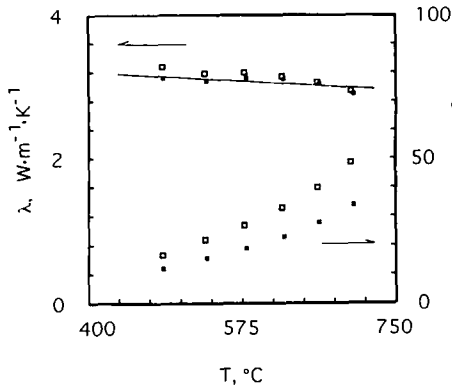


Fig. 9. Thermal conductivity of Pyroceram 9606 and temperature difference between the two faces: (□) 3.15 mm thick; (■) 2.1 mm thick.

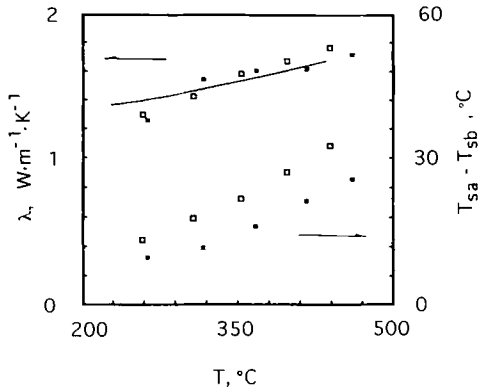


Fig. 10. Thermal conductivity of Pyrex 7740 and temperature difference between the two faces: (□) 5.0 mm thick; (■) 3.0 mm thick.

not perfectly canceled in Eq. (5) because the temperatures of the heater and the front surface of the specimen are not the same for the two cases, although the temperatures of the thermocouple junction are the same.

5. CONCLUSION

A new method for noncontact thermal conductivity measurement based on thermal radiation calorimetry (TRAC) was performed for a disk-shaped insulating specimen. Noncontact temperature measurements of both surfaces of the specimen were performed with pyrometers and a thermocouple set in the gap between a flat heater and a specimen. The resultant values deviate by about 5% from the recommended values for Pyroceram 9606 and Pyrex 7740.

ACKNOWLEDGMENTS

The author is indebted to T. Matsumoto of the National Research Laboratory of Metrology, Tsukuba, Japan, for his useful discussion on the thermal conductivity of reference substances and for his kind supply of Pyroceram 9606 for the present investigation.

REFERENCES

1. K. Hisano and T. Yamamoto, in *Proc. 12th Japan Symp. Thermophys. Prop., Vol. 12* (Kyoto, 1991), p. 287.
2. K. Hisano and T. Yamamoto, *High Temp. High Press.* **25**:337 (1993).

3. A. E. de Burr, *Rev. Sci. Instrum.* **19**:569 (1948).
4. J. H. Hong and T. Baba, *Proc. 2nd Asian Thermophys. Prop. Conf.* (Sapporo, 1989), p. 179.
5. L. C. Hulstrom, R. P. Tye, and S. E. Smith, *Proc. 19th Int. Conf. Therm. Conduct., Vol. 19* (Plenum Press, New York, 1987), pp. 199-211.
6. R. W. Powell, C. Y. Ho, and P. E. Liley, *National Standard Reference Data Series—National Bureau of Standard-8* (Nov. 25, 1966).